17. Pollitz, F. F. & Dixon, T. H. GPS measurements across the northern Caribbean plate boundary zone; impact of postseismic relaxation following historic earthquakes. *Geophys. Res. Lett.* **25,** 2233–2236 (1998).
18. Ambraseys, N. N. & Finkel, C. F.in *Historical Seismograms and Earthquakes of the World* (eds Lee, W. H. K., Meyers, H. & Shimazaki, K.), 173–180 (Academic, San Diego, 1988).
19. Dieterich, J. A constitutive law for rate of earthquake production and its application to earthquake clustering. *J. Geophys. Res.* **99,** 2601–2618 (1994).
20. Sornette, A. & Sornette, D. Self organized criticality and earthquake. *Europhys. Lett.* **9,** 197 (1989).
21. Bowman, D. D. *et al.* An observational test of the critical earthquake concept. *J. Geophys. Res.* **103,** 24359–24372 (1998).
22. Okada, Y. Internal deformation due to shear and tensile fault in a half-space. *Bull. Seismol. Soc. Am.* **82,** 1018–1040 (1982).
23. Segall, P. & Harris, R. Slip deficit on the San Andreas Fault at Parkfield, California, as revealed by inversion of geodetic data. *Science* **233,** 1409–1413 (1986).

Supplementary information is available on *Nature*'s World-Wide Web site (http://www.nature.com) or as paper copy from the London editorial office of *Nature*.

Acknowledgements

We thank F. F. Pollitz and R. Harris for comments on the manuscript. This work was supported by the EEC FAUST programme and the INSU-CNRS PNRN programmes.

Correspondence and requests for materials should be addressed to A.H.-F. (e-mail: ferrari@princeton.edu).

Fine-scale heterogeneity in the Earth's inner core

John E. Vidale*† **& Paul S. Earle***

Earth and Space Science Department and Institute of Geophysics and Planetary Physics†, University of California at Los Angeles, Los Angeles, California 90095-1567, USA*

The seismological properties of the Earth's inner core have become of particular interest as we understand more about its composition and thermal state[1,2]. Observations of anisotropy and velocity heterogeneity in the inner core are beginning to reveal how it has grown and whether it convects[3,4]. The attenuation of seismic waves in the inner core is strong, and studies of seismic body waves[5,6] have found that this high attenuation is consistent with either scattering or intrinsic attenuation[5]. The outermost portion of the inner core has been inferred to possess layering and to be less anisotropic than at greater depths[7–10]. Here we present observations of seismic waves scattered in the inner core which follow the expected arrival time of the body-wave reflection from the inner-core boundary. The amplitude of these scattered waves can be explained by stiffness variations of 1.2% with a scale length of 2 kilometres across the outermost 300 km of the inner core. These variations might be caused by variations in composition, by pods of partial melt in a mostly solid matrix or by variations in the orientation or strength of seismic anisotropy.

Here we examine 12 earthquakes and 4 nuclear explosions in the distance range 58° to 73°. The events, listed in Table 1, were recorded on LASA (Large Aperture Seismic Array) between 1969 and 1975, and were less than 100 km deep. LASA consisted of up to 525 short-period vertical-component seismometers buried to a depth of 70 m and spread across an aperture of 200 km in Montana[11,12].

Our seismograms mostly extend from the P wave back past the P′P′ arrival, spanning more than half an hour. An arrival that is not explained by previously identified ray-paths appears near the predicted arrival time for PKiKP, which is the faint reflection from the boundary between the inner and outer core. Generally, the boundary between the inner and outer core appears locally flat and sharp[8,13,14]. Figure 1 shows the onset time, duration, and slowness of the energy incident on LASA in this interval. The image is the logarithmic average of slant stacks of the 16 events generated from the seismograms after they had been passed through a 1-Hz band-pass filter.

We attribute the 200 s of observed ground motion to inner-core scattering (ICS) (Fig. 1). This energy arrives nearly vertically from the direction of the inner core. The energy builds for a few tens of seconds, then gradually fades back into the more omnidirectional background. Most of the energy lies between –0.02 and 0.02 s km^{-1}, consistent with paths from the inner core. The initial tens of seconds of the ICS have an average slowness near 0.01 s km^{-1}, close to that expected for PKiKP. These unexpected arrivals are not visible in the seismograms without stacking. PKiKP is barely visible, as expected at these distances[8,14,15].

Also visible in Fig. 1 is a comparable amount of energy with the same slowness as the direct P wave, which also fades with time. This late-arriving P coda is scattered near the event. LASA is sufficiently dense and wide to clearly distinguish between the inner-core arrivals and the P coda. The background noise is generated by the event; it diminishes monotonically with increasing time after the event, and is higher than the pre-event noise.

Our 16 events sample four distinct regions of the inner core (Fig. 2a). The ray paths of PKiKP and the ICS are shown in Fig. 2b. Many of the earthquakes occurred near Japan, and the explosions were in Novaya Zemlya; there were also earthquakes under Peru and

Table 1 Earthquakes and explosions in this study

Date dd/mm/yr	Time	Latitude (°N)	Longitude (°E)	Depth (km)	Distance
28/02/69	04:25:36.9	36.23	–10.48	33	68°
31/05/70	20:23:27.3	–9.18	–78.82	33	68°
02/08/71	07:24:56.0	41.37	143.44	45	73°
05/09/71	18:35:26.8	46.54	141.15	14	70°
06/09/71	13:37:10.1	46.76	141.39	21	70°
09/09/71	23:02:06.8	44.34	150.85	7	69°
27/09/71	05:59:55.8	73.39	54.92	0	59°
24/11/71	19:35:28.5	52.85	159.22	99	57°
28/02/73	06:37:54.4	50.51	156.58	62	60°
17/06/73	20:37:52.1	42.65	146.08	11	70°
24/06/73	02:43:22.8	43.29	146.43	26	70°
27/10/73	06:59:58:0	70.80	53.96	0	62°
15/05/74	18:59:56.1	49.98	156.22	58	60°
29/08/74	09:59:56.2	73.39	54.91	0	59°
09/10/74	07:32:00.6	44.64	150.09	34	67°
02/11/74	04:59:57.4	70.83	53.82	0	62°

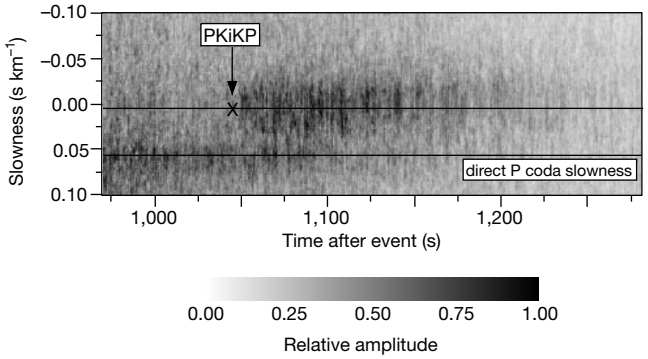

Figure 1 Average seismic-wave amplitude arriving between 970 and 1,280 s after all events. The image shows logarithmically averaged envelopes of the slant stacks for all 12 earthquakes and 4 nuclear explosions. The image shows the time and slowness, which is the reciporcal of apparent velocity, of energy incident on LASA. Three features of the signal are visible: (1) a stripe near 0.06 s km^{-1} slowness, which corresponds to late P coda and aftershocks, (2) a stripe of energy from 1,050 s until 1,250 s that we interpret as inner-core scattering (ICS), and (3) uniform background source-generated noise that diminishes with time. All subarrays are included in this stack for maximum slowness resolution.

near Iberia. The stack from each event shows ICS energy, although only by stacking all 16 events together do we find the fairly smooth envelope shown in Fig. 3.

We improve the signal-to-noise ratio of the stacks by excluding the outer three of the six rings of the LASA array, at the cost of reducing the high resolution in slowness from inclusion of all rings that is visible in Fig. 1. This winnowing left a 30-km array with more than 120 stations, and resulted in the cleanest stacks with sufficient slowness resolution to separate the ICS from the P coda. The reduced aperture also means that most of the energy incident from the direction of the inner core will stack coherently. In contrast, with the full array, only some of the energy from the inner core is fully in focus at each slowness and back-azimuth.

The amplitude of the ICS averages about 2% of the peak amplitude of PcP for the nuclear tests on 27 September 1971 and 29 August 1974 (Fig. 3). The other two explosions had clipped PcP arrivals, rendering them unsuitable for this calibration. Figure 3 also shows that the ICS lasts far longer than the source of the seismic radiation, which is a brief nuclear explosion. The small amplitude helps explain why ICS has not been previously identified. With an onset that requires 50 s to reach its peak and a signal so small that it cannot be seen in the individual seismograms, only a dense array can provide definitive proof of the strength of ICS. PKiKP is barely visible with amplitude of 3% of PcP, close to its expected value, which is very small because of a small inner-core boundary reflection coefficient[8,14].

Figure 4a compares the ICS envelope with the background noise from the inner three rings of LASA stacked for all 16 events. Figure 4b shows the ICS envelope after removing an estimate of uniform background noise. It is clear that the ICS starts near the calculated time for PKiKP, but that it takes 50 s to grow to its peak. PKiKP itself is only weakly visible for three events, and does not stand out in the stack.

As ICS has not been previously identified, and its presence implies strong fine-scale structure in the inner core, we have extensively explored possible alternative explanations. The high-frequency content indicates incident P waves, the small slowness indicates near-vertical propagation from the direction of the inner core, and the long travel time indicates a long path. We have failed to identify viable alternatives to ICS; PcPPcP (a double reflection from the core–mantle boundary) and P scattering to PKP at the core–mantle boundary come the closest to consistency with the ICS phase.

The calculated envelope of ICS for 1.2% r.m.s. variations in both density and elastic parameters and μ, with a correlation distance of 2 km, is shown in Fig. 4b. (Here is Lamé's parameter, and μ is the shear modulus.) Our observation geometry requires scattering angles near 90°, which is most sensitive to variations in , but variations in μ and density are not well resolved. Our three-dimensional calculation assumes single scattering[16] with equations modified to account for the non-Poisson velocity ratio v_P/v_S of the inner core (v_P and v_S are the velocities of P- and S-waves, respectively). Heterogeneities are parametrized by an exponential autocorrelation function. The elastic structure of the PREM model, with a value of seismic attenuation Q_P of 360 (ref. 6), is assigned throughout the inner core. Without attenuation in the inner core, the ICS would take about 100 s to rise to its peak and last 350 s, until its termination by the reflection from the far side of the inner core. However, the low Q_P in the inner core has the effect that only the scattering from the upper few hundred kilometres of the inner core survives to be seen. So our results only apply to the outer 300 km of the inner core; the deeper scattering structure is unresolved.

Assigning formal error bounds to our model parameters is difficult, given the trade-off between scale-length, r.m.s. variations, inner-core Q, depth distribution of the scatterers, and choice of autocorrelation function. The scale-length of 2 km was chosen because it produces the maximum theoretical amplitude with a minimum r.m.s. variation. Thus, given our scattering model, 1.2% is a lower bound on the r.m.s. variation. Our purpose is to demonstrate that a physically reasonable model exists that fits the data, adding strong support to our hypothesis of fine-scale structure within the inner core.

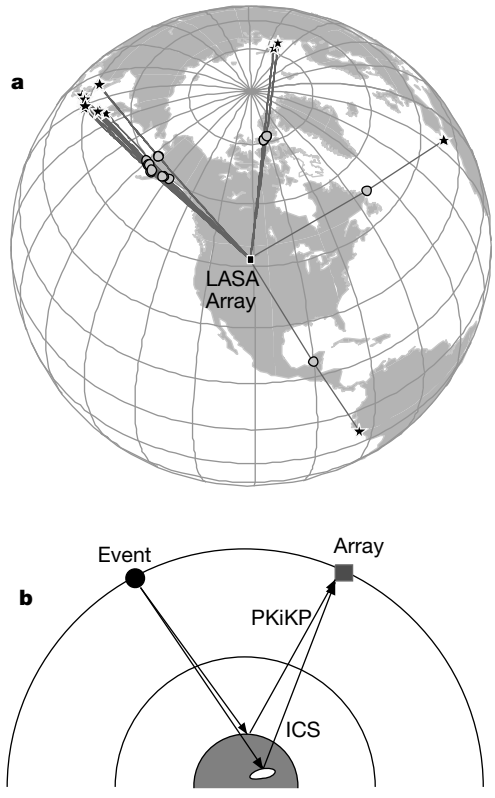

Figure 2 Location map of explosions, earthquakes, LASA, and midpoints of ray-paths. **a,** Map of events (stars), LASA (square), and the surface projection of the PKiKP reflection points (circles) on the inner-core boundary. **b,** Cross-section showing the ray paths of PKiKP and ICS.

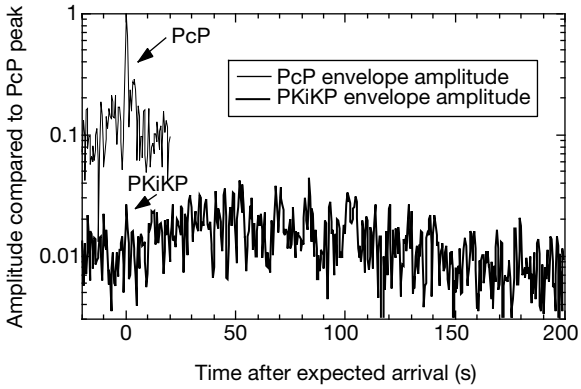

Figure 3 Comparison of ICS with PcP for the 27 September 1971 and 29 August 1974 nuclear tests. Both phases have been aligned with respect to their calculated arrival time. The PcP envelopes are averaged from 0.031 to 0.035 s km^{-1} and the ICS envelopes are averaged from 0.002 to 0.006 to suppress noise. Each event is coherently stacked, then an envelope is taken and the two events are averaged together. The record sections for the two events are very similar, consistent with the reported locations of the explosions being within 400 m.

The Born single-scattering approximation is valid for cases in which the energy loss due to scattering is small. Following Aki and Richards[17] (equation 13.53), and considering only the outer 300 km of the inner core that contributes to ICS waves, we obtain a fractional energy loss of around 10% for our preferred model.

It is difficult to estimate the scattering Q of our inferred heterogeneity in the inner core because we do not well constrain μ and density variations. Q_P at 1 Hz is seen in this study, and in other body-wave work[5,6], to be near 300. Normal mode analyses[18,19] imply higher Q_P, which translates to a less-attenuating core. It is plausible that the attenuation from scattering by fine-scale elastic structure is responsible for the discrepancy, because the normal modes would not be attenuated by such structure.

This magnitude of heterogeneity has several possible explanations. Variation in the orientation of anisotropy may lead to large apparent velocity variations. Some studies predict large variations in the compressional-wave velocity with propagation direction[20,21], although other studies predict far less variation[22]. The work we report here precludes the possibility that the inner core is a single crystal of iron, which would exhibit less scattering[22]. One-dimensional models of small-scale textural anisotropy show that about 8% velocity variation on a scale length of 1.2 km can explain the attenuation of PKIKP[5], although intrinsic attenuation was given as an alternative possibility. The present study requires scattering, and finds that three-dimensional heterogeneity fits ICS much better than one-dimensional layering.

A variable degree of partial melt may also play a role. The measured seismic shear-wave velocities of the core[18] are too slow to match laboratory measurements on pure iron[20]. This discrepancy may be due either to near-melting softening or to impurities accompanying iron that reduce shear velocity, like sulphur[23]. Because the inner core is probably nearly adiabatic, short-wavelength lateral variations in the degree of softening would probably be caused by variations in composition, which could lead to variations in melting point[24].

The ICS energy that we report here could be used to determine the rotation rate of the inner core with high precision: this could be achieved if sufficiently dense array recordings of similar sources, repeated at long time intervals, were analysed. This is possible because the scattered-wave travel times are much more sensitive to the movement of heterogeneities than are the transmitted-wave travel times that are currently used to estimate rotation rate[25]. □

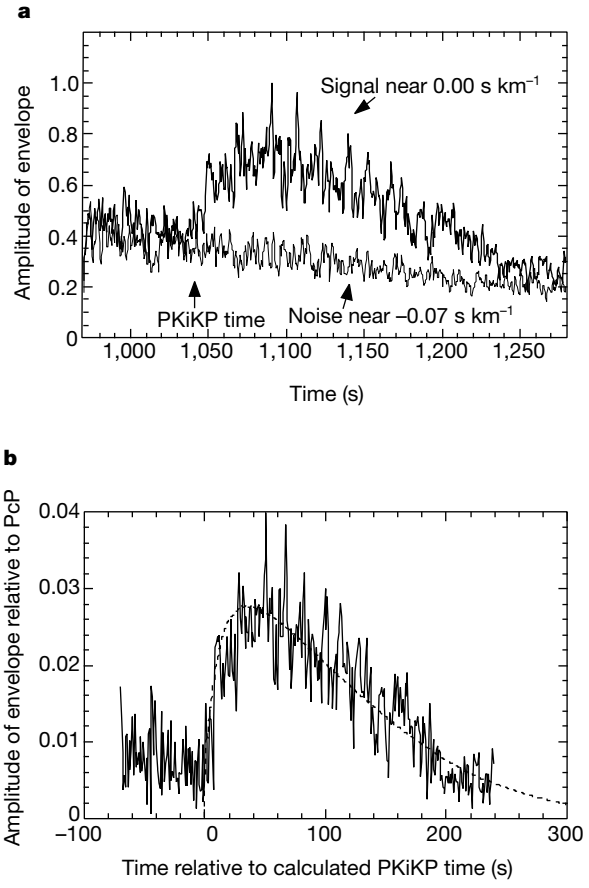

Figure 4 Stacks of inner-core scattering and noise amplitude. Only the three inner subarrays have been included in these stacks. **a,** The inner-core scattering, an average of the ten stacks between –0.005 and +0.005 s km^{-1}, is marked by the heavy line. The background noise, an average of the 10 stacks between –0.065 and –0.075 s km^{-1}, where discrete arrivals are not expected or observed, is marked by the thin line. **b**, An estimate of the inner-core scattering after removing noise at the level of the –0.07 s km^{-1} line in **a**. The noise is removed by squaring the heavy 0.0 s km^{-1} trace in **a**, subtracting the square of a straight line fit to the noise, and taking the square root. Superimposed is the scattering envelope calculated for our best-fitting model of heterogeneity (dashed line), which has 1.2% variations in the elastic parameters λ and μ, and density, with 2-km wavelength uniformly distributed across the inner core. PREM elastic velocity structure and a Q of 360 are used in our calculation.

Received 2 August 1999; accepted 25 January 2000.

1. Anderson, O. L. Mineral physics of iron and of the core. *Rev. Geophys.* **33,** 429–441 (1995).
2. Boehler, R. Temperatures in the Earth's core from melting point measurements of iron at high static pressures. *Nature* **363,** 534–536 (1993).
3. Tanaka, S. & Hamaguchi, H. Degree one heterogeneity and hemispherical variation in anisotropy in the inner core from PKP(BC) - PKP(DF) times. *J. Geophys. Res.* **102,** 2925–2938 (1997).
4. Romanowicz, B., Li, X. D. & Durek, J. Anisotropy in the inner core—could it be due to low-order convection. *Science* **274,** 963–966 (1996).
5. Cormier, V. F., Xu, L. & Choy, G. L. Seismic attenuation in the inner core: Viscoelastic or stratigraphic? *Geophys. Res. Lett.* **21,** 4019–4022 (1998).
6. Bhattacharyya, J., Shearer, P. M. & Masters, T. G. Inner core attenuation from short period PKP(BC) versus PKP(DF) waveforms. *Geophys. J. Int.* **114,** 1–11 (1993).
7. Song, X. & Helmberger, D. V. Seismic evidence for an inner core transition zone. *Science* **282,** 924–927 (1998).
8. Souriau, A. & Souriau, M. Ellipticity and density at the inner core boundary from subcritical PKiKP and PcP data. *Geophys. J. Int.* **98,** 39–54 (1989).
9. Shearer, P. M. Constraints on inner core anisotropy from PKP(DF) travel times. *J. Geophys. Res.* **99,** 19647–19659 (1994).
10. Song, X. & Helmberger, D. V. Depth dependence of anisotropy of Earth's inner core. *J. Geophys. Res.* **100,** 9805–9816 (1995).
11. Capon, J. Analysis of Rayleigh-wave multipath at LASA. *Bull. Seismol. Soc. Am.* **60,** 1701–1731 (1970).
12. Green, P. E., Frosch, R. A. & Romney, C. F. Principles of an experimental large aperture seismic array (LASA). *Proc. IEEE* **53,** 1821–1833 (1965).
13. Engdahl, E. R., Flinn, E. A. & Romney, C. F. Seismic waves reflected from the Earth's inner core. *Nature* **228,** 852–853 (1970).
14. Shearer, P. M. & Masters, T. G. The density and shear velocity contrast at the inner core boundary. *Geophys. J. Int.* **102,** 491–498 (1990).
15. Buchbinder, G. G. R., Wright, C. & Poupinet, G. Observations of PKiKP at distances less than 110°. *Bull. Seismol. Soc. Am.* **63,** 1699–1707 (1973).
16. Wu, R. -S. & Aki, K. Elastic wave scattering by a random medium and the small-scale inhomogeneities in the lithosphere. *J. Geophys. Res.* **90,** 10261–10273 (1985).
17. Aki, K. & Richards, P. G. *Quantitative Seismology: Theory and Methods* Vols 1 and 2 (Freeman, San Francisco, 1980).
18. Dziewonski, A. M. & Anderson, D. L. Preliminary reference Earth model. *Phys. Earth Planet Inter.* **25,** 297–356 (1981).
19. Widmer, R., Masters, T. G. & Gilbert, F. Spherically-symmetric attenuation within the Earth from normal mode data. *Geophys. J. Int.* **104,** 541–553 (1991).
20. Mao, H.-k. *et al.* Elasticity and rheology of iron above 220 GPa and the nature of the Earth's inner core. *Nature* **396,** 741–732 (1998).
21. Mao, H.-k. *et al.* Correction—Elasticity and rheology of iron above 220 GPa and the nature of the Earth's inner core. *Nature* **399,** 280 (1999).
22. Stixrude, L. & Cohen, R. E. High-pressure elasticity of iron and the anisotropy of the Earth's core. *Science* **267,** 1972–1975 (1995).
23. Jephcoat, A. & Olson, P. Is the inner core of the Earth pure iron? *Nature* **325,** 332–335 (1987).
24. Jeanloz, R. The nature of the Earth's core. *Annu. Rev. Earth Planet. Sci.* **18,** 357–386 (1990).
25. Song, X. D. & Richards, P. G. Seismological evidence for differential rotation of the Earth's inner core. *Nature* **382,** 221–224 (1996).

Acknowledgements

We thank the Albuquerque Seismological Laboratory and specifically R. Woodward and H. Bolton for access to LASA data; we also thank P. Shearer, F. Xu, S. Persh and J. Green for comments on the manuscript. L. Knopoff generalized the formula for scattering to non-Poisson solids.

Correspondence and requests for materials should be addressed to J.E.V. (e-mail: vidale@ucla.edu).